Carcinogenesis vol.34 no.12 pp.2750–2756, 2013
doi:10.1093/carcin/bgt286
Advance Access publication August 29, 2013

Genome-wide methylation analysis shows similar patterns in Barrett's esophagus and esophageal adenocarcinoma

Enping Xu[1,2], Jian Gu[1,*], Ernest T.Hawk[3], Kenneth K.Wang[4], Maode Lai[2], Maosheng Huang[1], Jaffer Ajani[5,†] and Xifeng Wu[1,†]

[1]Department of Epidemiology, The University of Texas MD Anderson Cancer Center, Houston, TX 77030, USA, [2]Department of Pathology, School of Medicine, Zhejiang University, Hangzhou, Zhejiang 310058, China, [3]Division of Cancer Prevention and Population Sciences, The University of Texas MD Anderson Cancer Center, Houston, TX 77030, USA, [4]Division of Gastroenterology and Hepatology, Mayo Clinic, Rochester, MN 55905, USA and [5]Department of Gastrointestinal Medical Oncology, Division of Cancer Prevention and Population Sciences, The University of Texas MD Anderson Cancer Center, Houston, TX 77030, USA

*To whom correspondence should be addressed. Department of Epidemiology, Unit 1340, The University of Texas MD Anderson Cancer Center, 1155 Pressler Street, Houston, TX 77030, USA. Tel: +713 792 8016; Fax: +713 745 1165;
Email: jiangu@mdanderson.org

Barrett's esophagus (BE) is a precursor of esophageal adenocarcinoma (EAC). To identify novel tumor suppressors involved in esophageal carcinogenesis and potential biomarkers for the malignant progression of BE, we performed a genome-wide methylation profiling of BE and EAC tissues. Using Illumina's Infinium HumanMethylation27 BeadChip microarray, we examined the methylation status of 27 578 CpG sites in 94 normal esophageal (NE), 77 BE and 117 EAC tissue samples. The overall methylation of CpG sites within the CpG islands was higher, but outside of the CpG islands was lower in BE and EAC tissues than in NE tissues. Hierarchical clustering analysis showed an excellent separation of NE tissues from BE and EAC tissues; however, the clustering of BE and EAC tissues was less clear, suggesting that methylation occurs early during the progression of EAC. We confirmed many previously reported hypermethylated genes and identified a large number of novel hypermethylated genes in BE and EAC tissues, particularly genes encoding ADAM (A Disintegrin And Metalloproteinase) peptidase proteins, cadherins and protocadherins, and potassium voltage-gated channels. Pathway analysis showed that a number of channel and transporter activities were enriched for hypermethylated genes. We used pyrosequencing to validate selected candidate genes and found high correlations between the array and pyrosequencing data (rho > 0.8 for each validated gene). The differentially methylated genes and pathways may provide biological insights into the development and progression of BE and become potential biomarkers for the prediction and early detection of EAC.

Introduction

Esophageal cancer is a highly aggressive malignancy. In the USA, there will be an estimated 17 990 new cases and 15 210 deaths in 2013 (1). Despite advances in treatment for patients with esophageal cancer, the 5 year overall survival rate remains <20% because most patients are diagnosed with advanced stage disease (2). Survival rates for patients with esophageal cancer could be improved if more patients were diagnosed at an early and potentially curable stage. Therefore, it is critical to identify clinically applicable biomarkers that can be used for the early detection and targeted prevention of esophageal cancer.

Abbreviations: ADAM, A Disintegrin And Metalloproteinase; BE, Barrett's esophagus; EAC, esophageal adenocarcinoma; NE, normal esophageal; ROC, receiver operating characteristic.

[†]These authors are co-last authors of this study.

The two major histological types of esophageal cancer, esophageal squamous cell carcinoma and esophageal adenocarcinoma (EAC), have striking geographic differences in their incidences: esophageal squamous cell carcinoma is predominant in Asian countries, whereas EAC is the most rapidly increasing solid tumor in the Western world and currently accounts for ~80% of new esophageal cancer cases in the USA (3,4). Barrett's esophagus (BE) is the precursor lesion of EAC in which the squamous epithelial cells in the esophageal mucosa are replaced by premalignant columnar epithelial cells. BE is the most important risk factor for the development of EAC. The incidence of EAC in patients with BE is 30–100 times higher than in the general population (5–7). However, a recent large population-based cohort study estimated that the risk of malignant progression in BE patients is 0.22% per year (8). This low absolute risk of progression calls for more accurate risk stratification in BE patients for better informed preventive and/or therapeutic interventions. Independent objective biomarkers are needed to complement and enhance risk stratification of BE patients based on pathological grading.

It is now widely recognized that epigenetic alterations are associated with the process of neoplastic transformation (9). DNA methylation is one of the most important epigenetic alterations and plays a critical role in the development of human malignancies (10). Promoter regions are usually enriched with CpG dinucleotides, known as CpG islands (11,12); hypermethylation of these islands is associated with transcriptional repression of tumor suppressor genes, whereas hypomethylation is associated with increased expression of oncogenes (13–16). The identification of specific DNA methylation sites could not only provide significant biological insights into the development and progression of cancer but also discover novel biomarkers for early detection, diagnosis and prognosis of cancer (17,18). To identify novel biomarkers during the malignant progression of BE, in this study, we performed a genome-wide methylation profiling in a large series of BE and EAC tissues in comparison with normal esophageal (NE) tissues.

Materials and methods

Human tissue samples

A total of 117 EAC tissue samples, 77 BE tissue samples and 94 samples of adjacent NE tissue from the surrounding esophagus were included in this study. The EAC, BE and NE tissues were collected as described previously (19–21). All tissues were snap frozen at the time of diagnostic or therapeutic endoscopic biopsies using a tissue collection protocol approved by the institutional review board. Experienced pathologists performed histologic readings of the corresponding juxtaposed paraffin-fixed specimens. Only those with >70% tumor cells (for EAC tissue) or metaplasia/dysplasia (for BE tissue) were included in this study. All tissues were from patients diagnosed as having EAC. A corresponding normal squamous tissue sample was collected from a healthy appearing mucosa at least 3 cm from the edge of the apparent tumor from each patient by a gastroenterologist. All tumors were staged according to the criteria in the sixth edition of the 'American Joint Commission on Cancer' Atlas (22).

DNA extraction and bisulfite conversion

Genomic DNA was extracted using a QIAamp DNeasy Blood and Tissue Kit (Qiagen, Valencia, CA) according to the manufacturer's instructions. DNA concentration was assessed with an ND-1000 spectrophotometer (NanoDrop Technologies, Wilmington, DE) and the average fragment length was assessed by gel electrophoresis. Bisulfite conversion of genomic DNA from each sample was done using the EZ DNA Methylation Kit (Zymo Research, Orange, CA), which converts unmethylated cytosines to uracil but leaves methylated cytosines unchanged.

Genome-wide methylation assay

Bisulfite-converted genomic DNA was analyzed using Illumina's Infinium Human Methylation27 BeadChip Kit (San Diego, CA). This array targets

27 578 unique CpG sites located within the proximal promoter regions of the transcription start sites of 14 495 genes. The methylation profiling was performed according to the manufacturer's protocol. Briefly, ~200 ng of bisulfite-converted DNA was applied per chip. During hybridization, the DNA molecules were annealed to two different bead types with locus-specific DNA oligomers—one for the methylated locus and another for the unmethylated locus. The single-base extension of the probes incorporated a labeled dideoxynucleoside triphosphate, which was subsequently stained with a fluorescence reagent. The methylation status of each interrogated CpG site was then calculated as the β value, defined as ratio of the fluorescent signals from the methylated allele to the sum of the methylated and unmethylated alleles. The β value is a quantitative measure of DNA methylation levels of specific CpGs and ranges from 0 (completely unmethylated) to 1 (completely methylated).

Validation of Infinium methylation platform by pyrosequencing

The methylation change of the five differentially methylated genes between NE and BE samples were validated by pyrosequencing, a sequencing-by-synthesis method that quantitatively monitors the real-time incorporation of nucleotides through the enzymatic conversion of released pyrophosphate into a proportional light signal. After bisulfite treatment and PCR, the degree of methylation of each CpG position in a sequence was determined from the ratio of thymine to cytosine. We used the Vacuum Prep Tool (Qiagen) to prepare single-stranded PCR products according to manufacturer's instructions. Pyrosequencing was performed using a PyroMark Q96 System (Qiagen) according to manufacturer's protocol.

Statistical analysis

We used Bead Studio Methylation Module software (Illumina) to assess the differences in methylation levels for different samples and groups. The results from pyrosequencing and the β values from the methylation assay were correlated using the Spearman rank correlation. A supervised hierarchical cluster analysis was performed using the average linkage method. All statistical tests were two-sided. For all tests, $P < 0.05$ was used as the level of significance. The DAVID bioinformatics tool (23,24) was used to determine the enrichment of individual gene ontology terms and to map genes onto the Kyoto Encyclopedia of Genes and Genomes pathway maps. The enriched gene ontology terms were reported as clusters to reduce redundancy. The *P* value for each cluster is the geometric mean of the *P* value for all the gene ontology categories in the cluster. Benjamini–Hochberg multiple testing correction was used to control false discovery rate.

Results

Overall methylation profiles of NE, BE and EAC tissues

We assessed the methylation status of 27 587 CpG sites across 14 495 genes in a total of 288 esophageal tissues (94 NE, 77 BE and 117 EAC). Prior to determining differential methylation, we removed probes that failed in any one of the samples ($n = 68$) and probes in chromosomes X and Y ($n = 1092$). As described previously (25,26), we also removed those probes with β values in all samples being ≥0.8 or ≤0.2 to reduce the number of non-variable sites from subsequent analyses ($n = 8689$). This resulted in a final data set of 17 729 probes for further analysis. Within this probe set, 10 836 CpG were within CpG islands and 6893 CpG were outside CpG islands. Comparison of mean β values revealed no differences in overall CpG methylation in the NE, BE and EAC tissue samples (Table I). However, when CpG island and non-CpG island sites were analyzed separately, we found significant differences between the distributions of methylation profiling in the NE, BE and EAC tissue samples. Within the CpG islands, the overall methylation (mean β values of all sites) in NE tissue was significantly lower than the BE and EAC tissues. In contrast, outside CpG islands, the overall methylation in NE tissue was significantly higher than the BE and EAC tissues.

Hierarchical clustering of NE, BE and EAC tissues

We performed a supervised hierarchical clustering to differentiate these tissues (Figure 1). We first randomly split all the samples into a discovery and a validation set. We selected the top 10 differentially methylated CpG sites with the smallest *P* values of mean β value difference between each pair-wise comparison of tissues (i.e. BE versus NE, EAC versus NE and EAC versus BE) and used them to cluster corresponding tissues. The clustering of NE tissues from BE and EAC tissues was excellent; however, the clustering of BE and EAC tissues was much less clear (Figure 1A–C). When we used the same 10 CpG sites to cluster tissues in the validation set, there was again excellent clustering of NE from BE or EAC tissues, but the BE and EAC tissues were interspersed (Figure 1D–F).

Receiver operating characteristic curve

To further evaluate the value of the methylated CpG sites in discriminating BE and EAC from normal tissues, we constructed a receiver operating characteristic (ROC) curve by plotting sensitivity versus specificity (Figure 2) using the top 10 differentially methylated CpG sites. The area under the ROC curve, a commonly used indicator for estimating the diagnostic efficacy of a potential biomarker, was calculated. For discriminating BE from NE tissues, the area under the ROC curve was 0.965 (sensitivity: 94.81%, specificity: 91.49%), and for discriminating EAC from NE tissues, the area under the ROC curve was 0.973 (sensitivity: 94.87%, specificity: 93.62%), suggesting the excellent value of these differentially methylated CpG sites in discriminating BE or EAC tissues from NE tissues.

Table I. DNA methylation profiling of samples from normal, BE and EAC tissues

Variable	*N*	NE	BE	EAC	P^*	P^{**}	P^{***}
		Mean (SD)	Mean (SD)	Mean (SD)			
All CpG sites	17 729						
Discover set		38.1 (29.5)	38.2 (28.5)	38.2 (28.2)	0.74	0.58	0.82
Validation set		38.0 (29.6)	38.2 (28.5)	38.3 (28.3)	0.52	0.35	0.76
Combined set		38.0 (29.5)	38.2 (28.5)	38.3 (28.2)	0.63	0.45	0.79
CpG sites inside CpG island	10 836						
Discover set		25.0 (25.1)	27.7 (25.6)	27.4 (25.2)	8.20E-15	1.22E-12	0.48
Validation set		24.8 (25.2)	27.3 (25.4)	27.1 (25.0)	5.27E-13	1.54E-11	0.60
Combined set		24.9 (25.1)	27.5 (25.4)	27.3 (25.1)	6.95E-14	4.19E-12	0.54
CpG sites outside CpG island	6893						
Discover set		58.6 (23.7)	54.7 (24.9)	55.2 (23.9)	1.67E-21	7.82E-17	0.18
Validation set		58.7 (23.5)	55.3 (24.5)	55.8 (24.0)	1.23E-16	1.31E-12	0.21
Combined set		58.7 (23.6)	55.0 (24.7)	55.5 (24.0)	5.57E-19	1.12E-14	0.20

SD, standard deviation.
$^*P$ values for the difference between NE tissue and BE tissue.
$^{**}P$ values for the difference between NE tissue and EAC tissue.
$^{***}P$ values for the difference between BE tissue and EAC tissue.

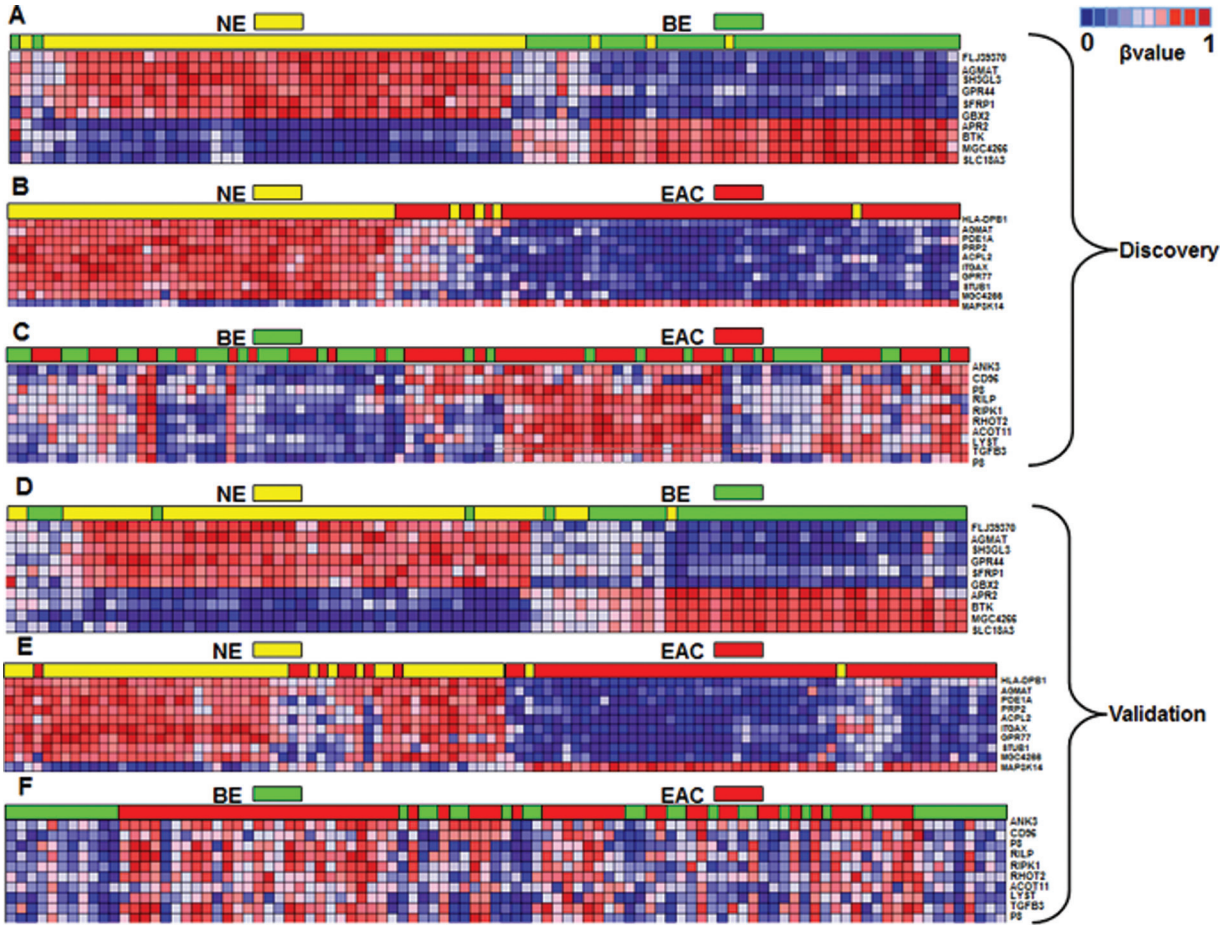

Fig. 1. Supervised hierarchical clustering of 10 CpG sites in (**A**) NE tissues with EAC tissues in the discovery set, (**B**) NE tissues with BE tissues in the discovery set, (**C**) EAC with BE tissues in the discovery set, (**D**) NE tissues with EAC tissues in the validation set, (**E**) NE tissues with BE tissues in the validation set and (**F**) EAC with BE tissues in the validation set. Each column represents a sample and each row represents a CpG site. Methylation levels vary from fully unmethylated (blue) to fully methylated (red).

Differentially methylated CpG sites and host genes in BE/EAC tissues

There were a large number of differentially methylated individual CpG sites between NE and BE/EA tissues. Of particular interest are those sites within CpG islands that had low methylation ($\beta < 0.2$) in NE tissues but showed significant hypermethylation ($\beta > 0.5$) in BE/EA tissues. The host genes of these hypermethylated CpG sites are potential tumor suppressors. Tables II and III showed the top 20 hypermethylated CpG sites and host genes from pair-wise comparison of BE versus NE and EAC versus NE, respectively. All these CpG sites showed consistent hypermethylation in both BE and EAC tissues, among which SFRP1 (27), GBX2 (28), ADAM12 (29), PTGDR (30), DMRT1 (31), PTPRT (32), SH3GL3 (33), LAMA1 (34), COL15A1 (35) and AJAP1 (36,37) have been reported previously to be hypermethylated in various cancers. In addition to these top 20 CpG sites, a complete examination of those differentially methylated CpG sites found several interesting gene families: ADAM (A Disintegrin And Metalloproteinase) and ADAMTS (ADAM with Thrombospondin Motifs) peptidase family, cadherins and protocadherins, and potassium voltage-gated channels (Supplementary Table 1, available at *Carcinogenesis* Online).

We also compared the methylation status of EAC tissues with that of BE tissues (Supplementary Table 2, available at *Carcinogenesis* Online). There were no CpG sites that fit the same criteria set previously (i.e. $\beta < 0.2$ in BE tissues but $\beta > 0.5$ in EAC tissues).

There were also many hypomethylated CpG sites in pair-wise comparison of BE versus NE, EAC versus NE and EAC versus BE (Supplementary Tables 3–5, available at *Carcinogenesis* Online), most of which were likely resulted from global hypomethylation in neoplastic tissues.

Validation of differentially methylated CpG sites by pyrosequencing

The methylation of the five differentially methylated CpG sites between NE and BE tissues in the discovery set (SLC18A3, CACNB2, SH3GL3, CHRNA3 and SFRP1; Table II) was validated by pyrosequencing after bisulfite conversion. There was a strong correlation between the methylation levels of each CpG site as assayed by these two methods (rho > 0.8 for each one; Table IV), demonstrating technical reproducibility of the Illumina array method. Pyrosequencing is a highly specific method with little non-specific noise. Therefore, the methylation level detected by pyrosequencing was generally lower than that detected by the Illumina array.

Pathway analysis of hypermethylated genes

We then used the DAVID bioinformatics tool to explore the potential pathways involved in EAC development using 107 hypermethylated genes ($\beta < 0.2$ in NE tissues and $\beta > 0.5$ in BE/EA tissues). The hypermethylated genes were enriched for genes involved in cell adhesion, cell motion, cell surface receptor-linked signal transduction, cell–cell signaling, regulation of transcription and so on (Supplementary Table 6, available at *Carcinogenesis* Online). The top significant Kyoto Encyclopedia of Genes and Genomes pathways included transcriptional activity, sequence-specific DNA binding, and a number of channel and transporter activities.

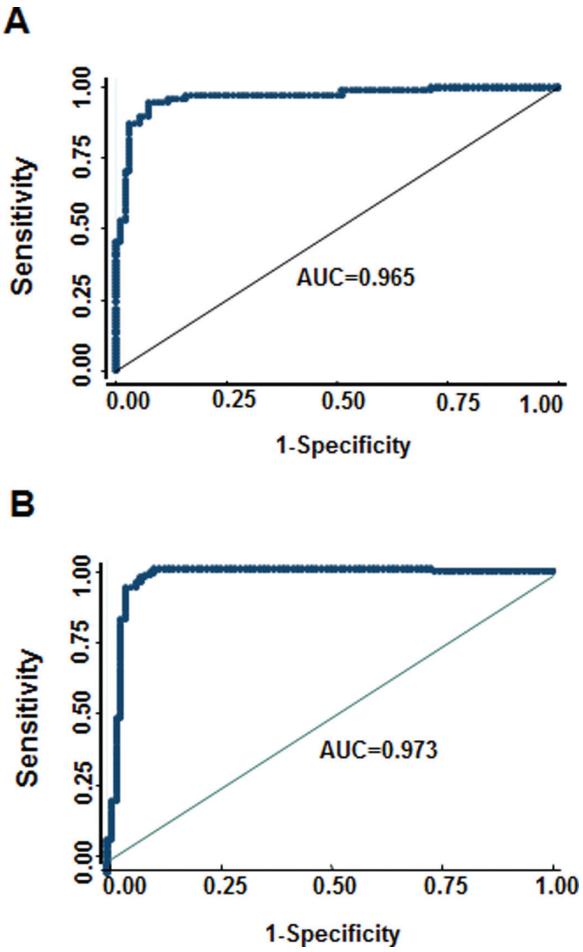

Fig. 2. ROC curve analysis of the diagnostic efficacy of 10 common differentially methylated CpG sites in BE and EAC in all samples. (**A**) ROC curve for discriminating NE tissues from BE. (**B**) ROC curve for discriminating NE tissues from EAC. AUC, area under the ROC curve.

Discussion

Carcinogenesis of EAC involves a multistep process from intestinal metaplasia to low- and high-grade dysplasia and finally to adenocarcinoma (38). It is well known that epigenetic events are involved in this process. Two distinct DNA methylation alterations play fundamental roles in cancer development: global hypomethylation and regional hypermethylation of tumor suppressor genes (9,10,15). In this study, we found that within the CpG islands, the overall methylation in BE and EAC tissues was significantly higher than that in normal tissues. The CpG islands are considered the most relevant for expression of the corresponding gene, and hypermethylation of these islands is associated with transcriptional repression of tumor suppressor genes. The similar findings in the other tumor type have been reported (34,39). On the other hand, we found that the overall methylation outside CpG islands in BE and EA tissues was significantly lower than that in normal tissues. Unlikely CpG sites inside CpG islands, CpG sites outside CpG islands are usually not involved in regulating gene expression. The methylation level outside CpG islands reflects more of global methylation than specific gene promoter methylation. These data are consistent with literature that global hypomethylation and promoter hypermethylation of specific tumor suppressor genes are both involved in the development of BE and EAC (40–42).

Our hierarchical clustering analysis showed an excellent separation of NE tissues from BE and EAC tissues; however, the clustering of BE and EAC tissues was less clear. In addition, we could find numerous individual CpG sites that showed low methylation ($\beta < 0.2$) in normal tissues but were hypermethylated ($\beta < 0.5$) in BE and EAC tissues; however, there was not a single CpG site that had low methylation ($\beta < 0.2$) in BE tissues but was hypermethylated ($\beta < 0.5$) in EAC tissues. None of the hypomethylated CpG sites in EAC compared with BE had a decreased β value of >0.2 (Supplementary Table 5, available at *Carcinogenesis* Online). These observations suggest that hypermethylation occurs early during the progression of EAC and plays a more prominent role in driving metaplasia and dysplasia formation than carcinoma development. Similar to our results, Smith *et al.* (43) compared the methylation of nine known hypermethylated genes in NE, BE and EAC tissue samples and demonstrated high similarity of aberrant DNA methylation in BE and EAC. Taken together, these data support that BE is a pre-cancerous lesion with profound molecular alterations that are similar to carcinoma.

The identified individual hypermethylated CpG sites and host genes are of particular interests because these genes are candidate tumor suppressor genes for BE and EAC development. Among the top differentially hypermethylated genes in BE/EAC tissues (Tables II and III), several genes have been reported previously to be hypermethylated in BE/EAC tissues and other cancers, such as SFRP1 (27), whereas many others, including GBX2 (28), ADAM12 (29), PTGDR (30), DMRT1 (31), PTPRT (32), SH3GL3 (33), LAMA1 (34), COL15A1 (35) and AJAP1 (36,37), were reported in other cancers. For new hypermethylated genes, membrane transporter and ion channel genes were unusually frequent, including genes encoding SLC18A3 (a vesicular amine transporter), CACNB2 (a voltage-dependent calcium channel), CHRNA3 (a ligand-gated ion channel), SLC6A2 (a multipass membrane transporter of sodium and neurotransmitter; Table II) and the simultaneous hypermethylation of a large number of potassium-gated channels (Supplementary Table 1, available at *Carcinogenesis* Online). It is also interesting that many channel and transporter pathways were enriched for hypermethylated genes (Supplementary Table 7, available at *Carcinogenesis* Online). It is tempting to speculate that chronic exposure to bile acid may cause physiological and pathological changes of the membrane transporters and channels, which may contribute to metaplasia. Another notable observation was the high frequent simultaneous hypermethylation of genes encoding cell matrix and cell adhesion proteins, such as COL5A1 (collagens), AJAP1 (an adherens junction-associated protein), LAMA1 (a laminin; Tables II and III) and a large number ADAM, ADAMTS, cadherins and protocadherins (Supplementary Table 1, available at *Carcinogenesis* Online). The hypermethylation of some of these genes is likely involved in cellular histology and morphology changes because the BE tissues are columnar compared with the squamous nature of normal tissues.

Among the newly identified hypermethylated genes, IRX4 is a homeobox transcription factor, and a recent study showed that it can suppress prostate cancer cell growth through the interaction with vitamin D receptor and there was a significant interaction between IRX4 and vitamin D receptor in their reciprocal transcriptional regulation (44). PTPRT is the most frequently mutated protein tyrosine phosphatase in human cancers and can suppress colorectal cancer cell growth (45).

The Illumina methylation array constitutes a robust platform that produces reliable and highly reproducible data. It has been compared with other platforms by previous studies and has shown consistent results, with correlations ranging consistently >0.8 (46). Our correlation study of the five differentially methylated CpG sites between Illumina's array data and pyrosequencing data supports the technical reliability of Illumina's array platform. The recapitulation of most previously reported hypermethylated genes further support the reproducibility of this technology. Illumina's Methylation27 assay detects the methylation status of ~2 CpG sites per gene for most genes. For genes with multiple CpG loci on the array, we found all the loci to be differentially methylated in the same direction. One recent study that used the same platform to analyze DNA methylation changes during long-term culture of mesenchymal stromal cells found that closely positioned CpGs on the microarray revealed very similar methylation patterns (47). These observations suggest that aberrant methylations are not restricted to an individual CpG site but rather affect nearby CpG sites and the entire CpG islands.

Table II. The top 20 hypermethylated CpG sites in BE versus NE tissues

Target ID	Symbol	Discovery set (β value)			Validation set (β value)		
		NE	BE	EAC	NE	BE	EAC
		Mean (SD)	Mean (SD)	Mean (SD)	Mean (SD)	Mean (SD)	Mean (SD)
cg22946150	*SH3GL3*	8.6 (15.2)	59.0 (18.2)	57.8 (19.9)	7.1 (11.5)	52.9 (25.2)	56.5 (19.2)
cg06954481	*GBX2*	15.1 (16.8)	66.2 (18.6)	60.6 (21.3)	16.6 (15.2)	56.8 (23.0)	56.4 (24.4)
cg11389172	*SLC18A3*	12.1 (14.5)	54.9 (15.6)	56.4 (15.7)	12.0 (11.6)	50.2 (20.1)	54.2 (12.4)
cg10362591	*SLC6A2*	14.1 (15.8)	63.0 (18.9)	58.6 (20.2)	14.5 (13.6)	57.6 (24.4)	56.6 (22.1)
cg01805540	*CACNB2*	11.6 (15.2)	57.3 (17.4)	57.2 (18.3)	9.9 (11.5)	52.5 (20.4)	56.5 (15.5)
cg26024843	*COL5A1*	12.8 (14.0)	52.0 (14.3)	50.6 (13.4)	12.9 (12.2)	47.6 (17.2)	49.3 (14.7)
cg08045570	*FOXF2*	6.8 (12.3)	51.0 (19.9)	53.8 (19.5)	6.0 (9.2)	44.6 (23.6)	47.3 (20.4)
cg13168820	*PTPRT*	11.6 (13.3)	53.3 (17.3)	56.7 (17.0)	11.1 (10.5)	48.2 (21.7)	54.9 (14.2)
cg09516965	*PTGDR*	10.6 (13.3)	57.4 (20.9)	54.3 (26.7)	10.2 (12.5)	45.8 (27.9)	53.9 (23.9)
cg04603031	*CHRNA3*	16.6 (14.2)	56.8 (15.5)	53.8 (19.0)	16.0 (11.5)	51.3 (17.0)	53.2 (16.9)
cg27269921	*MN1*	9.6 (14.2)	52.3 (17.5)	42.2 (23.6)	9.5 (14.3)	40.2 (22.6)	40.9 (24.3)
cg01988129	*ADHFE1*	19.3 (15.4)	65.2 (18.6)	66.2 (19.4)	19.1 (12.1)	60.3 (22.3)	61.6 (18.4)
cg19001226	*HOXD1*	15.5 (12.4)	53.1 (15.5)	49.1 (18.9)	12.7 (10.5)	46.5 (20.5)	44.7 (17.9)
cg09083627	*SLITRK5*	11.1 (14.1)	51.9 (16.3)	53.7 (15.4)	9.5 (9.7)	45.6 (20.5)	50.6 (16.0)
cg17457560	*NRG1*	14.4(11.9)	53.4 (17.3)	47.9 (20.3)	12.8 (11.6)	46.7 (20.3)	50.3 (16.9)
cg03963198	*IRX4*	17.2 (15.2)	58.7 (16.0)	59.1 (15.7)	15.9 (12.6)	53.1 (20.3)	56.4 (15.2)
cg15839448	*SFRP1*	13.7 (12.8)	50.6 (15.3)	50.7 (15.4)	12.3 (10.2)	45.2 (19.6)	48.2 (14.0)
cg13398291	*SFRP1*	12.9 (13.9)	56.0 (19.0)	53.4 (19.6)	10.8 (9.3)	50.5 (24.7)	52.9 (17.7)
cg26599006	*GSCL*	11.3 (14.6)	53.3 (17.6)	52.9 (19.3)	9.3 (10.7)	44.1 (23.1)	48.2 (21.1)
cg07846220	*LAMA1*	18.2 (16.5)	61.8 (16.8)	62.3 (14.3)	15.5 (14.1)	56.6 (21.0)	61.6 (14.1)

SD, standard deviation.

Table III. The top 20 hypermethylated CpG sites in EAC versus NE tissues

Target ID	Symbol	Discovery set (β value)			Validation set (β value)		
		NE	BE	EAC	NE	BE	EAC
		Mean (SD)	Mean (SD)	Mean (SD)	Mean (SD)	Mean (SD)	Mean (SD)
cg17892556	*ZNF625*	12.3 (14.4)	58.0 (27.6)	64.2 (19.8)	10.6 (10.6)	53.7 (30.7)	57.6 (22.5)
cg13168820	*PTPRT*	11.6 (13.3)	53.3 (17.3)	56.7 (17.0)	11.1 (10.5)	48.2 (21.7)	54.9 (14.2)
cg04434339	*ST6GAL2*	10.0 (14.2)	51.2 (18.0)	55.3 (16.5)	9.0 (10.2)	47.4 (22.4)	52.8 (14.9)
cg11389172	*SLC18A3*	12.1 (14.5)	54.9 (15.6)	56.4 (15.7)	12.0 (11.6)	50.2 (20.1)	54.2 (12.4)
cg07846220	*LAMA1*	18.2 (16.5)	61.8 (16.8)	62.3 (14.3)	15.5 (14.1)	56.6 (21.0)	61.6 (14.1)
cg09083627	*SLITRK5*	11.1 (14.1)	51.9 (16.3)	53.7 (15.4)	9.5 (9.7)	45.6 (20.5)	50.6 (16.0)
cg12300353	*KCTD8*	10.6 (13.4)	50.4 (19.4)	53.1 (16.1)	10.9 (11.4)	46.8 (24.1)	47.9 (18.9)
cg17525406	*AJAP1*	18.1 (16.9)	65.0 (20.4)	66.9 (17.5)	15.6 (12.5)	60.1 (24.4)	64.9 (16.4)
cg08045570	*FOXF2*	6.8 (12.3)	51.0 (19.9)	53.8 (19.5)	6.0 (9.2)	44.6 (23.6)	47.3 (20.4)
cg07080358	*C2orf32*	8.1 (14.3)	51.9 (26.1)	59.1 (20.9)	5.7 (10.5)	48.8 (28.8)	53.4 (21.7)
cg19018097	*FLJ30934*	8.3 (12.2)	46.7 (20.9)	52.3 (18.2)	8.2 (15.1)	43.3 (22.5)	50.2 (17.4)
cg26024843	*COL5A1*	12.8 (14)	52.0 (14.3)	50.6 (13.4)	12.9 (12.2)	47.6 (17.2)	49.3 (14.7)
cg03168582	*DMRT1*	8.3 (13.5)	53.0 (26.3)	56.6 (20.1)	6.4 (11.1)	46.9 (28.4)	53.4 (19.6)
cg17108819	*CD8A*	10.8 (14.2)	53.5 (23.5)	59.3 (19.9)	8.7 (11.3)	49.6 (26.9)	56.8 (17.1)
cg04034767	*GRASP*	13.4 (12.6)	51.2 (26.1)	60.8 (20.2)	11.7 (10)	47.6 (28.1)	50.8 (22.6)
cg22946150	*SH3GL3*	8.6 (15.2)	59.0 (18.2)	57.8 (19.9)	7.1 (11.5)	52.9 (25.2)	56.5 (19.2)
cg03963198	*IRX4*	17.2 (15.2)	58.7 (16)	59.1 (15.7)	15.9 (12.6)	53.1 (20.3)	56.4 (15.2)
cg09229912	*CUTL2*	16.4 (18.5)	61.6 (18.1)	63.4 (16.5)	14.3 (14.9)	56.9 (23.5)	60.8 (15.9)
cg19884262	*FLJ46831*	13.0 (13.8)	53.8 (17.6)	55.5 (17.2)	12.5 (12.1)	50.1 (21.8)	52.7(15.6)
cg11668923	*ADAM12*	12.1 (16.1)	59.0 (21.7)	61.8 (20.1)	10.1 (11.3)	55.4 (26.4)	58.5 (20.0)

SD, standard deviation.

The major strength of this study was the large sample size of samples. There were 288 tissue samples included in this study, making this study one of the largest whole-genome methylation array studies. There are a few limitations to this study. First, this is a cross-sectional study to compare one time collection of tissues from different individuals. All the BE tissues in this study were obtained from patients who have developed EAC. It is possible that these BE tissues may have more rampant methylation aberrations than tissues from BE patients in the general population who would never develop EAC. Future prospective studies are warranted to compare methylation in BE patients who develop and those who do not develop EAC to identify predictive biomarkers for BE progression.

In conclusion, this large-scale study provides strong evidence that DNA methylation plays an important role in the development of BE and EAC. The methylation pattern of BE and EAC is remarkably similar. The differentially methylated genes identified in this study may provide biological insights into the development and progression of BE and become potential biomarkers for the prediction and early detection of EAC.

Supplementary material

Supplementary Tables 1–7 can be found at http://carcin.oxfordjournals.org/

Table IV. Correlations between DNA methylation levels analyzed by pyrosequencing and by methylation array

Variables	No.	Array analysis (β value)			Pyrosequencing (% of methylated C)			Rho
		NE	BE	EAC	NE	BE	EAC	
		Mean (SD)	Mean (SD)	Mean (SD)	Mean (SD)	Mean (SD)	Mean (SD)	
SLC18A3	37	12.04 (13.09)	52.51 (18.06)	55.27 (14.14)	16.10 (4.77)	47.10 (11.88)	42.80 (18.60)	0.87
CACNB2	33	10.75 (13.44)	54.85 (19.01)	56.85 (16.89)	0.72 (0.80)	31.75 (16.16)	30.94 (21.93)	0.85
SH3GL3	36	7.82 (13.43)	55.92 (22.08)	57.14 (19.46)	4.60 (4.71)	42.47 (12.23)	38.50 (18.97)	0.92
CHRNA3	41	16.28 (12.84)	53.97 (16.42)	53.54 (17.88)	1.37 (1.58)	30.59 (14.87)	32.32 (20.93)	0.87
SFRP1	40	22.06 (13.86)	60.64 (15.74)	61.26 (12.49)	1.59 (3.06)	40.48 (15.37)	37.15 (21.11)	0.85

SD, standard deviation.

Funding

National Institutes of Health (CA111922 and CA138671); the Premalignant Genome Atlas Program of the Duncan Family Institute for Cancer Prevention and Risk Assessment at The University of Texas MD Anderson Cancer Center; MD Anderson Cancer Center Start-up Fund (to J.G.).

Conflict of Interest Statement: None declared.

References

1. Siegel,R. *et al.* (2013) Cancer statistics, 2013. *CA. Cancer J. Clin.*, **63**, 11–30.
2. Montgomery,E. *et al.* (2001) Reproducibility of the diagnosis of dysplasia in Barrett esophagus: a reaffirmation. *Hum. Pathol.*, **32**, 368–378.
3. Hongo,M. *et al.* (2009) Epidemiology of esophageal cancer: Orient to Occident. Effects of chronology, geography and ethnicity. *J. Gastroenterol. Hepatol.*, **24**, 729–735.
4. Lagergren,J. (2005) Adenocarcinoma of oesophagus: what exactly is the size of the problem and who is at risk? *Gut*, **54** (suppl. 1), i1–i5.
5. Wild,C.P. *et al.* (2003) Reflux, Barrett's oesophagus and adenocarcinoma: burning questions. *Nat. Rev. Cancer*, **3**, 676–684.
6. Shaheen,N.J. *et al.* (2009) Barrett's oesophagus. *Lancet*, **373**, 850–861.
7. Jankowski,J.A. *et al.* (2002) Esophageal adenocarcinoma arising from Barrett's metaplasia has regional variations in the west. *Gastroenterology*, **122**, 588–590.
8. Bhat,S. *et al.* (2011) Risk of malignant progression in Barrett's esophagus patients: results from a large population-based study. *J. Natl. Cancer Inst.*, **103**, 1049–1057.
9. Feinberg,A.P. *et al.* (2004) The history of cancer epigenetics. *Nat. Rev. Cancer*, **4**, 143–153.
10. Jones,P.A. *et al.* (2002) The fundamental role of epigenetic events in cancer. *Nat. Rev. Genet.*, **3**, 415–428.
11. Bird,A. (2002) DNA methylation patterns and epigenetic memory. *Genes Dev.*, **16**, 6–21.
12. Takai,D. *et al.* (2002) Comprehensive analysis of CpG islands in human chromosomes 21 and 22. *Proc. Natl Acad. Sci. USA*, **99**, 3740–3745.
13. Herman,J.G. *et al.* (2003) Gene silencing in cancer in association with promoter hypermethylation. *N. Engl. J. Med.*, **349**, 2042–2054.
14. Cui,H. *et al.* (2002) Loss of imprinting in colorectal cancer linked to hypomethylation of H19 and IGF2. *Cancer Res.*, **62**, 6442–6446.
15. Jones,P.A. *et al.* (2007) The epigenomics of cancer. *Cell*, **128**, 683–692.
16. Long,C. *et al.* (2007) Promoter hypermethylation of the RUNX3 gene in esophageal squamous cell carcinoma. *Cancer Invest.*, **25**, 685–690.
17. Cheng,Y.Y. *et al.* (2007) Frequent epigenetic inactivation of secreted frizzled-related protein 2 (SFRP2) by promoter methylation in human gastric cancer. *Br. J. Cancer*, **97**, 895–901.
18. Yu,J. *et al.* (2009) Methylation of protocadherin 10, a novel tumor suppressor, is associated with poor prognosis in patients with gastric cancer. *Gastroenterology*, **136**, 640–51.e1.
19. Luthra,R. *et al.* (2006) Gene expression profiling of localized esophageal carcinomas: association with pathologic response to preoperative chemoradiation. *J. Clin. Oncol.*, **24**, 259–267.
20. Luthra,M.G. *et al.* (2007) Decreased expression of gene cluster at chromosome 1q21 defines molecular subgroups of chemoradiotherapy response in esophageal cancers. *Clin. Cancer Res.*, **13**, 912–919.
21. Gu,J. *et al.* (2010) Genome-wide catalogue of chromosomal aberrations in Barrett's esophagus and esophageal adenocarcinoma: a high-density single nucleotide polymorphism array analysis. *Cancer Prev. Res. (Phila).*, **3**, 1176–1186.
22. Singletary,S.E. *et al.* (2003) Classification of isolated tumor cells: clarification of the 6th edition of the American Joint Committee on Cancer Staging Manual. *Cancer*, **98**, 2740–2741.
23. Huang da,W. *et al.* (2009) Systematic and integrative analysis of large gene lists using DAVID bioinformatics resources. *Nat. Protoc.*, **4**, 44–57.
24. Huang da,W. *et al.* (2009) Bioinformatics enrichment tools: paths toward the comprehensive functional analysis of large gene lists. *Nucleic Acids Res.*, **37**, 1–13.
25. Byun,H.M. *et al.* (2009) Epigenetic profiling of somatic tissues from human autopsy specimens identifies tissue- and individual-specific DNA methylation patterns. *Hum. Mol. Genet.*, **18**, 4808–4817.
26. Fryer,A.A. *et al.* (2011) Quantitative, high-resolution epigenetic profiling of CpG loci identifies associations with cord blood plasma homocysteine and birth weight in humans. *Epigenetics*, **6**, 86–94.
27. Zou,H. *et al.* (2005) Aberrant methylation of secreted frizzled-related protein genes in esophageal adenocarcinoma and Barrett's esophagus. *Int. J. Cancer*, **116**, 584–591.
28. Bell,A. *et al.* (2011) CpG island methylation profiling in human salivary gland adenoid cystic carcinoma. *Cancer*, **117**, 2898–2909.
29. Rahmatpanah,F.B. *et al.* (2009) Large-scale analysis of DNA methylation in chronic lymphocytic leukemia. *Epigenomics*, **1**, 39–61.
30. Spisák,S. *et al.* (2012) Genome-wide screening of genes regulated by DNA methylation in colon cancer development. *PLoS One*, **7**, e46215.
31. Jee,C.D. *et al.* (2009) Identification of genes epigenetically silenced by CpG methylation in human gastric carcinoma. *Eur. J. Cancer*, **45**, 1282–1293.
32. Laczmanska,I. *et al.* (2013) Protein tyrosine phosphatase receptor-like genes are frequently hypermethylated in sporadic colorectal cancer. *J. Hum. Genet.*, **58**, 11–15.
33. Fang,W.J. *et al.* (2012) Genome-wide analysis of aberrant DNA methylation for identification of potential biomarkers in colorectal cancer patients. *Asian Pac. J. Cancer Prev.*, **13**, 1917–1921.
34. Kim,Y.H. *et al.* (2011) Epigenomic analysis of aberrantly methylated genes in colorectal cancer identifies genes commonly affected by epigenetic alterations. *Ann. Surg. Oncol.*, **18**, 2338–2347.
35. Morris,M.R. *et al.* (2010) Identification of candidate tumour suppressor genes frequently methylated in renal cell carcinoma. *Oncogene*, **29**, 2104–2117.
36. Lin,N. *et al.* (2012) Deletion or epigenetic silencing of AJAP1 on 1p36 in glioblastoma. *Mol. Cancer Res.*, **10**, 208–217.
37. Matsusaka,K. *et al.* (2011) Classification of Epstein-Barr virus-positive gastric cancers by definition of DNA methylation epigenotypes. *Cancer Res.*, **71**, 7187–7197.
38. Fléjou,J.F. (2005) Barrett's oesophagus: from metaplasia to dysplasia and cancer. *Gut*, **54** (Suppl 1), i6–i12.
39. Duong,C.V. *et al.* (2012) Quantitative, genome-wide analysis of the DNA methylome in sporadic pituitary adenomas. *Endocr. Relat. Cancer*, **19**, 805–816.
40. Kaz,A.M. *et al.* (2011) DNA methylation profiling in Barrett's esophagus and esophageal adenocarcinoma reveals unique methylation signatures and molecular subclasses. *Epigenetics*, **6**, 1403–1412.
41. Alvarez,H. *et al.* (2011) Widespread hypomethylation occurs early and synergizes with gene amplification during esophageal carcinogenesis. *PLoS Genet.*, **7**, e1001356.
42. Alvi,M.A. *et al.* (2013) DNA methylation as an adjunct to histopathology to detect prevalent, inconspicuous dysplasia and early-stage neoplasia in Barrett's esophagus. *Clin. Cancer Res.*, **19**, 878–888.

43. Smith,E. *et al.* (2008) Similarity of aberrant DNA methylation in Barrett's esophagus and esophageal adenocarcinoma. *Mol. Cancer*, **7**, 75.
44. Nguyen,H.H. *et al.* (2012) IRX4 at 5p15 suppresses prostate cancer growth through the interaction with vitamin D receptor, conferring prostate cancer susceptibility. *Hum. Mol. Genet*., **21**, 2076–2085.
45. Wang,Z. *et al.* (2004) Mutational analysis of the tyrosine phosphatome in colorectal cancers. *Science*, **304**, 1164–1166.
46. Oster,B. *et al.* (2011) Identification and validation of highly frequent CpG island hypermethylation in colorectal adenomas and carcinomas. *Int. J. Cancer*, **129**, 2855–2866.
47. Bork,S. *et al.* (2010) DNA methylation pattern changes upon long-term culture and aging of human mesenchymal stromal cells. *Aging Cell*, **9**, 54–63.

Received March 15, 2013; revised July 15, 2013; accepted August 16, 2013